

Water Resources Research



RESEARCH ARTICLE

10.1029/2024WR039155

Monsoon and Glacial Meltwater Input Drive Seasonal Cooling of a Himalayan Ice-Contact Lake

Key Points:

- Lake surface temperatures exceeded 9°C at the surface, and were consistently warmer close to the glacier front, driven by convection
- Monsoon-specific meteorological conditions and input of glacial meltwater drove vertical mixing, resulting in overall lake cooling
- Monsoon-influenced ice-contact lakes experience shortened summer stratification period, likely reducing lake-induced glacier melt

Supporting Information:

Supporting Information may be found in the online version of this article.

Correspondence to:







A. C. Scoffield,
gyacs@leeds.ac.uk

Citation:

Scoffield, A. C., Quincey, D. J., Kerr, N. R., Rowan, A. V., Carrivick, J. L., Woolway, R. I., et al. (2025). Monsoon and glacial meltwater input drive seasonal cooling of a Himalayan ice-contact lake. *Water Resources Research*, 61, e2024WR039155. <https://doi.org/10.1029/2024WR039155>

Received 10 OCT 2024

Accepted 23 OCT 2025

Alex C. Scoffield¹ , Duncan J. Quincey¹, Nicky R. Kerr¹, Ann V. Rowan² , Jonathan L. Carrivick¹ , R. Iestyn Woolway³ , Nawraj Khanal⁴ , C. Scott Watson¹ , and Simon J. Cook⁵

¹School of Geography and water@leeds, University of Leeds, Leeds, UK, ²Department of Earth Science, University of Bergen & Bjerknes Centre for Climatic Research, Bergen, Norway, ³School of Ocean Sciences, Bangor University, Bangor, UK, ⁴Central Department of Hydrology and Meteorology, Tribhuvan University, Kathmandu, Nepal, ⁵Division of Geography and Environmental Science and UNESCO Centre for Water Law, Policy and Science, University of Dundee, Dundee, UK

Abstract Thousands of glacial lakes exist across the Himalaya. However, the physical characteristics of these lakes that drive changes in glacier mass balance and meltwater delivery downstream are poorly understood. We measured water temperature with depth in Thulagi Lake, Nepal, between May and October 2023 to give the first observations of the thermal dynamics of a Himalayan ice-contact glacial lake spanning the entirety of the glacier melt season. During the pre-monsoon and early monsoon periods, we observed lake temperatures greater than 9°C as high incoming shortwave radiation and wind-driven vertical mixing drove warming at the lake surface. Lake temperature consistently cooled with depth, indicating that the lake was stratified (74% of days within this period). However, these conditions were short lived, with a curtailed summer stratification period after which the lake cooled and vertical mixing was more common. During the pre-monsoon and early monsoon periods (May–July), consistently higher temperatures were measured near the glacier front than at distal locations (mean differences of 0.30°C–0.96°C at the lake surface) indicating intense convection and the delivery of heat to the ice front resulting in subaqueous melt. Our results show that monsoon conditions (increased precipitation, reduced incoming solar shortwave radiation and lower wind speed) and the input of glacial meltwater inhibit prolonged lake warming, suggesting that subaqueous melt-driven frontal ablation may play a less important role in driving glacier mass loss here than it does in other glacierised regions.

Plain Language Summary Himalayan glaciers form the headwaters of major South Asian rivers, including the Ganges, the Brahmaputra and the Indus rivers, and the quantity and timing of runoff is of great importance from both a human and ecological perspective. Glacier mass loss in the Himalaya has led to the formation of thousands of glacial lakes. Many lakes are in direct contact with glaciers (these are called lake-terminating glaciers), where the lake can enhance melting through direct ablation of the ice and by promoting calving. This study provides the first seasonal observations of lake temperature in the Himalaya at Thulagi Lake, Nepal. Early in the monsoon season, we observed lake surface temperatures greater than 9°C resulting from intense heating by the sun and windy conditions that drive mixing within the lake. During the monsoon season, the lake cooled both at the surface and the lake bottom, in direct contrast to observations from glacial lakes worldwide where warm surface conditions persist until the autumn. Our results show that monsoon conditions and input of glacial meltwater inhibit lake warming, suggesting that direct melting of glaciers by lake water is less important in driving glacier mass loss here than for glaciers in other climatic settings.

1. Introduction

Glacial lakes are increasing in number and expanding in size across the Himalaya, and this trend is expected to persist, or accelerate, as glaciers continue to lose mass in response to a warming climate (Furian et al., 2021; Shugar et al., 2020). Previous work has shown that ice-contact lakes can modify glacier geometry and ice flow (Sutherland et al., 2020) and promote greater ablation (King et al., 2018). Thus, these lakes play an important role in controlling future glacier mass loss and ice dynamics, and in modulating freshwater resources for downstream catchments (Brun et al., 2019; Carrivick et al., 2020; Zhang et al., 2023, 2024). The physical conditions of these lakes are understudied, in part due to their remote, high-elevation settings. This presents a major knowledge gap

© 2025. The Author(s).

This is an open access article under the terms of the [Creative Commons Attribution License](https://creativecommons.org/licenses/by/4.0/), which permits use, distribution and reproduction in any medium, provided the original work is properly cited.

that needs closing so that lake effects can be more fully incorporated into numerical modeling approaches that seek to predict future glacier change.

Long-term observations (months to years) demonstrate that ice-contact glacial lakes undergo a seasonal thermal cycle similar to non-ice-contact lakes, with two discrete periods (summer, winter) of stratification (i.e., dimictic; Ficker et al., 2017; Wells & Troy, 2022; Yang et al., 2018). During the summer stratification period, glacial lakes are often separated into two distinct layers, a warmer upper layer and a cold, turbid lower layer (Bird et al., 2022; Sharma et al., 2012; Sugiyama et al., 2016, 2021), separated by a thermocline which can inhibit vertical mixing (Woolway & Simpson, 2017). In situ observations from glacierised regions around the world indicate that high suspended sediment loads, attributed to subglacial discharge during the glacier melt season, may substantially impact the thermal regime of ice-contact glacial lakes (Carrivick & Tweed, 2013; Sugiyama et al., 2021). The high sediment loads of subglacial discharge in the cold, turbid lower layer induce a sediment-driven stratification pattern, which would otherwise be less dense than the overlying warmer water, as freshwater reaches its density maximum at 4°C (Lewis, 1983; Sugiyama et al., 2016).

Lakes are primarily influenced by two climatological factors which determine their vertical structure, surface heating (e.g., solar radiation) and drivers of mixing (e.g., wind speeds) (Chikita, 2007; Miles et al., 2016; Wang et al., 2023; Woolway & Simpson, 2017; Wüest et al., 2000). Typically, increased solar radiation and wind speeds during the summer lead to lake surface warming and a gradual deepening of the thermocline (Wells & Troy, 2022). Additionally, local climatological variations (e.g., seasonal wind patterns) and short-term meteorological events (e.g., precipitation, storms) may influence lake thermal regimes. For example, high wind speeds can cause complete mixing in stratified lakes dependent on the relative bathymetry (Jennings et al., 2012; Sugiyama et al., 2016, 2021). Furthermore, depending on the atmospheric conditions, precipitation can induce near-surface air cooling through evapotranspiration, or warming through condensation, and enhance mixing of the lake surface layer (Miles et al., 2016; Röhl, 2006). What is unknown however, is the influence of synoptic climate phenomena (e.g., monsoons) on the thermal regimes of Himalayan ice-contact glacial lakes.

Nepal's climate is strongly influenced by the Indian summer monsoon (ISM), which brings heavy, convective precipitation throughout the country between June and October each year (Kulkarni et al., 2011; Mukherjee et al., 2015). The ISM is a component of the South Asian summer monsoon, driven by differences in atmospheric pressure during summer which drive moisture transport from the Bay of Bengal in the Indian Ocean across the Himalayan land mass (Bookhagen et al., 2005; Brunello et al., 2020; Kulkarni et al., 2011; Mukherjee et al., 2015). The ISM has a longitudinal delay of approximately 15 days across the Himalaya, with a westerly continental progression during onset and an easterly oceanic progression during withdrawal, resulting in differing monsoon lengths by region (Brunello et al., 2020; Saha et al., 2023). The ISM can be defined by three broad phases: pre-monsoon and monsoon establishment (May–June), peak monsoon (July–August) and monsoon withdrawal (September–October) (Kulkarni et al., 2009).

Observations of thermal regimes from Himalayan ice-contact glacial lakes are scarce and cover only short periods (days to weeks). Piecing together independent pre-, peak- and post-monsoon observations (Chikita, 2007; Chikita et al., 1999, 2000, 2001; Watson et al., 2020) suggests that these lakes may be dimictic, similar to non-ice-contact glacial lakes in the region (Sharma et al., 2012), with clear stratification in both summer and winter, albeit driven by differing mechanisms (temperature- and sediment-driven regimes). However, the evolution of ice-contact glacial lake thermal conditions throughout the monsoon season is unknown. Given the unique climatological influence of the ISM during this period, observations from other regions are of limited value in understanding the characteristics of ice-contact glacial lakes in monsoon-influenced regions. These characteristics (e.g., lake temperature, circulation and topography) play a crucial role in glacier melt and calving rates, and consequently, ice dynamics (Benn et al., 2007; Chikita, 2007; Mallalieu et al., 2020; Röhl, 2006; Sakai et al., 2009; Warren & Kirkbride, 2003), representing a major challenge for future projections of glacier change. Here, the number, area and volume of glacial lakes is projected to increase, and thus, the role they play in driving glaciological and hydrological processes in this region will become more dominant (Zhang et al., 2023, 2024). We present the first seasonal measurements of ice-contact glacial lake temperature in the Himalayan region. We characterize both spatial and temporal variations in lake temperature throughout the glacier melt season, and interpret those results in the context of the monsoon, which we find drives a markedly different evolution in lake characteristics compared to non-ice-contact glacial lakes in the Himalaya and lakes in non-monsoon influenced regions of the world.

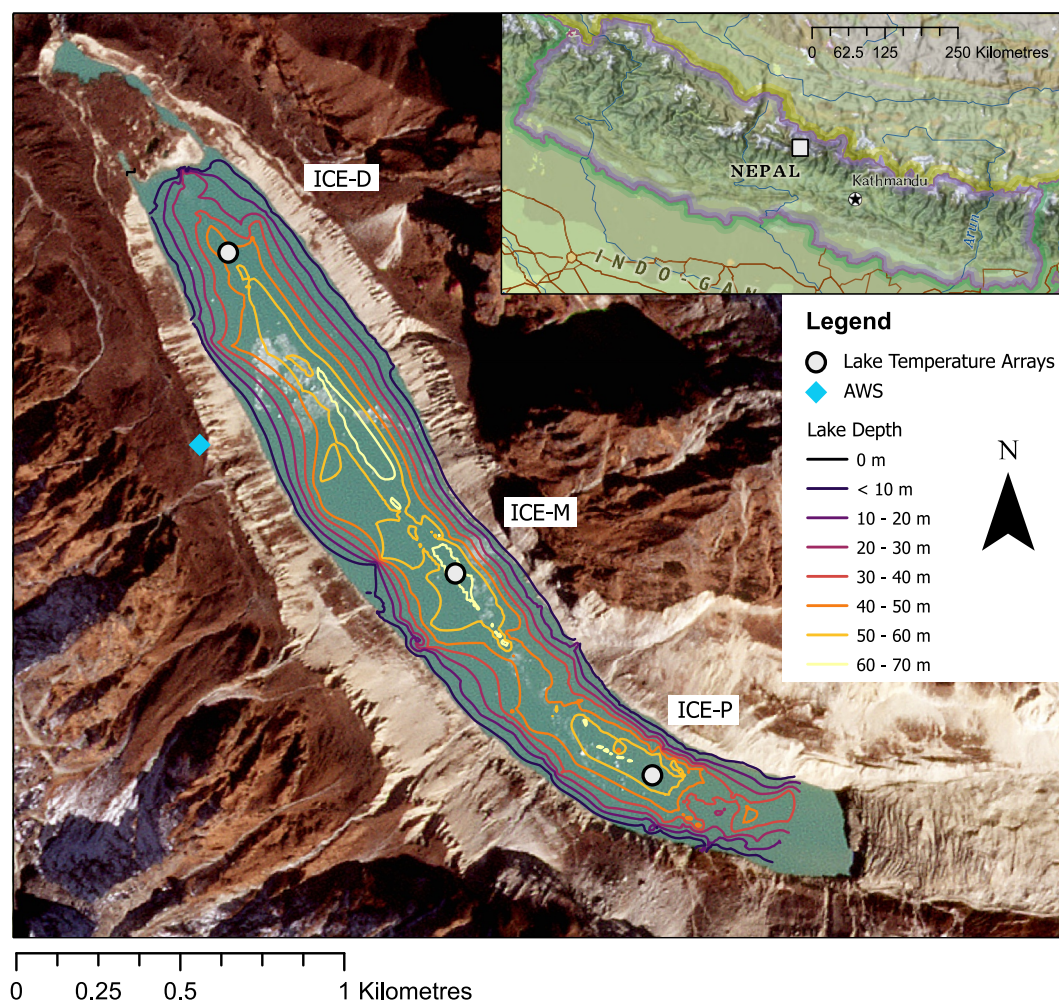


Figure 1. Map of Thulagi Lake, Nepal, including lake sensor (ICE-P, ICE-M and ICE-D) and automatic weather station (AWS) locations and observed lake bathymetry in May 2023. Background satellite image is from 16 November 2023 (Planet Labs Imagery).

2. Study Area

Thulagi Lake (known locally as Dona Lake) is a high-elevation moraine-dammed proglacial lake located adjacent to the Manaslu massif in the Mansiri Himal region of Nepal (4,050 m a.s.l.; Haritashya et al., 2018) (Figure 1). Thulagi Lake has increased in area by 18% since 1990–1999 to 0.93 km² in 2018 (Shugar et al., 2020; Watson et al., 2020). It was previously identified as moderate risk for a glacial lake outburst flood and its bathymetry is well known relative to other sites (Haritashya et al., 2018). Survey data acquired in 2017 suggest that the maximum depth of the lake was 76 m (Haritashya et al., 2018). Our bathymetric survey recorded a maximum depth of 79 m (Text S1 and Figure S1 in Supporting Information S1). Thulagi's bed morphology is characterized by a narrow longitudinal trough between 65 and 78 m deep, separated into sections by sills which we interpret to be submerged ice marginal moraines constructed during periods of relative terminus stability as the glacier receded.

A vertical temperature profile was measured for this lake during 28–30 October 2017 (mooring situated near ICE-D; Figure 1; Watson et al., 2020) and showed mean surface temperature of 2.6°C, with the warmest temperatures observed at the lake bottom (~55 m) demonstrating a reverse thermal gradient indicative of winter conditions at dimictic lakes (Wang et al., 2023). The cool surface temperatures were interpreted to reflect the impact of a large calving event and its subsequent melt during this observational period (Watson et al., 2020).

3. Methods

3.1. Lake Temperature Measurements

We measured three vertical temperature profiles in Thulagi Lake through the installation of moorings at ice-distal (ICE-D), ice-middle (ICE-M) and ice-proximal (ICE-P) locations from May to October 2023 (Figure 1). Each mooring consisted of six or seven temperature sensors dependent on lake depth suspended on static cord by buoys at the lake surface and anchored by a sandbag at the lakebed. Sensors were installed at the surface (~ 0.1 m deep), 1, 5, 10, 30 and 50 m, with an additional sensor at 70 m at the deepest sites. TinyTag TGC-0020 sensors were used at depths less than 15 m, while TinyTag Aquatic 2 sensors were used at depths greater than 15 m. Both models have a manufacturer accuracy rating of $\sim 0.50^{\circ}\text{C}$, but prior to deployment all of the sensors were calibrated in a controlled temperature environment at 4.5°C , which indicated a relative accuracy of 0.10°C (Watson et al., 2020). We therefore adopt this value as the uncertainty in our measurements since the consistency between sensors is considerably more important in our analysis than the absolute accuracy of any single temperature value. The measurements were acquired with intervals of 10 min over 148 days from 16 May 2023 to 10 October 2023. All sensors were recovered from ICE-D (surface to 50 m), while only shallow sensors were able to be recovered from ICE-M (surface to 5 m) and ICE-P (surface to 10 m). The inability to retrieve all sensors related to a mooring issue. The mooring set-up was designed to be retrieved from the surface (pulling up the sensors with the sandbag attached), but the volume of sediment that accumulated during the observation period prevented retrieval of the sandbag (and the sensors at depth).

The study aims to identify both spatial and temporal patterns in lake temperature, evaluating changes with lake depth, with increasing distance from the glacier terminus, and throughout the glacier melt season. Owing to the large amount of spatial (three locations at varying depths) and temporal (5 months at ten-minute intervals) data collected, effect size was used as the focus of the statistical analysis given that larger sample sizes are known to limit the accuracy of probability-based approaches (Klaar et al., 2020). Effect size was calculated using Cohen's D, which is the difference between the mean temperatures divided by the mean of their pooled standard deviation. Differences were considered to be significant where Cohen's D was >0.5 (medium effect) (Cohen, 1988; Klaar et al., 2020). Hourly and daily moving averages were calculated to suppress noise and allow analyses over varying temporal scales. Lake stratification was quantified by calculating the difference between the shallowest and deepest observations, where a difference greater than 1°C may be considered stratified (Read et al., 2011; Woolway et al., 2014).

3.2. Meteorological Observations

Meteorological conditions were measured using a custom automatic weather station (AWS) comprising of Campbell Scientific sensors, installed on the true left lateral moraine of Thulagi Lake at 4,143 m a.s.l (Figure 1). Air temperature (manufacturer rated accuracy of $\pm 0.1^{\circ}\text{C}$), relative humidity (manufacturer rated accuracy of $\pm 2.0\%$), wind speed (manufacturer rated accuracy of ± 0.5 m/s) and direction (manufacturer rated accuracy of $\pm 5^{\circ}$). Each variable was measured at thirty-minute intervals between 16 May 2023 and 19 August 2023. Incoming solar radiation (manufacturer rated accuracy of $\pm 5\%$ for daily total radiation) was measured at thirty-minute intervals between 16 May 2023 and 15 July 2023. Several of the meteorological data sets are incomplete because of livestock interference.

3.3. Monsoon Onset and Withdrawal

Due to the longitudinal delay of the ISM, regionally-specific monsoon onset and withdrawal dates are most relevant to analyze its effects at a specific site (i.e., Thulagi Lake). Here, we use the regional onset and withdrawal dates published annually by Nepal's Department for Hydrology and Meteorology (DHM, 2024), which agree well with the long-term mean onset dates calculated by Brunello et al. (2020) (10th June 2023, Brunello et al., 2020 vs. 14th June 2023, DHM, 2024).

4. Results

4.1. Lake Thermal Structure

Data describing the thermal structure of Thulagi Lake are presented in two parts. First, we focus on observations from the complete data set (surface, 1, 5, 10, 30, and 50 m) acquired at ICE-D to characterize the seasonal evolution

of the lake thermal structure, supported by the shallow observations we were able to gather from ICE-M and ICE-P. These observations are described in three temporal periods, May to June, July to August and September to October, in line with the trends in lake temperature throughout the 5-month data set. Secondly, we focus on the shallow observations (surface to 10 m) acquired at all sites to describe the longitudinal variability in lake thermal characteristics, and in particular how they differ in the ice-distal and ice-proximal locations of the lake.

4.1.1. Seasonal Evolution of Lake Thermal Structure

Observations at ICE-D show a consistent pattern of cooling with depth throughout the observation period (Figures 2a, 2b and 3). Mean monthly lake temperature peaked in June, at $6.1 \pm 0.1^\circ\text{C}$ at the lake surface and $4.5 \pm 0.1^\circ\text{C}$ at 50 m. Minimum mean monthly lake temperatures at 10 m ($3.2 \pm 0.1^\circ\text{C}$), 30 m ($3.0 \pm 0.1^\circ\text{C}$) and 50 m ($2.9 \pm 0.1^\circ\text{C}$) were observed in August, while those at the surface ($3.7 \pm 0.1^\circ\text{C}$) and 1 m ($3.6 \pm 0.1^\circ\text{C}$) were observed in September (Figure S2 in Supporting Information S1).

From the start of observations in May, daily mean lake surface temperature increased from $4.8 \pm 0.1^\circ\text{C}$ on 16th May to a maximum of $7.9 \pm 0.1^\circ\text{C}$ on 9th June. Daily mean lake temperatures at 50 m similarly increased throughout May and June to a maximum of $4.8 \pm 0.1^\circ\text{C}$ on 30th June. The maximum temperature recorded was $9.2 \pm 0.1^\circ\text{C}$ at the lake surface on 9th June. Lake temperatures at the surface, 1 and 10 m were similar throughout this period (i.e., followed a similar pattern), with mean diurnal temperature ranges of $2.3 \pm 0.1^\circ\text{C}$ at the surface, $1.9 \pm 0.1^\circ\text{C}$ at 1 m and $1.2 \pm 0.1^\circ\text{C}$ at 10 m (Figure S3 in Supporting Information S1). Lake temperatures below 30 m were also similar, but with considerably lower mean diurnal temperature ranges of $0.2 \pm 0.1^\circ\text{C}$ at 30 m and $0.2 \pm 0.1^\circ\text{C}$ at 50 m. Between 16th May and 30th June, the difference in mean daily temperature between the lake surface and 50 m was greater than 1°C for 34 out of the 46 days observed (74% of days), indicating that the lake was well stratified during this period.

Between July and August, lake temperatures at all depths cooled, reducing to a daily mean minimum of $3.3 \pm 0.1^\circ\text{C}$ at the lake surface (30th August) and $2.7 \pm 0.1^\circ\text{C}$ at 50 m (26th August). Lake temperatures displayed similar patterns during this period, with mean diurnal temperature ranges of $2.0 \pm 0.1^\circ\text{C}$ at the surface and $1.2 \pm 0.1^\circ\text{C}$ at 1 m. Lake temperatures at 10 m followed a similar pattern with those at 30 and 50 m during this period with mean diurnal temperature ranges of $0.4 \pm 0.1^\circ\text{C}$ at 10 m, $0.2 \pm 0.1^\circ\text{C}$ at 30 m and $0.1 \pm 0.1^\circ\text{C}$ at 50 m, respectively. The difference in mean daily temperature of the lake surface and 50 m was greater than 1°C for 35 out of 62 days between 1st July and 31st August (56%).

From September to October, lake temperatures warmed following the lake temperature minima observed in August. At all depths, lake temperatures were similar, with reduced mean diurnal temperature ranges of $1.4 \pm 0.1^\circ\text{C}$ at the lake surface and $0.6 \pm 0.1^\circ\text{C}$ at 1 m, in comparison to the previous time period (July and August). During this period, the difference in mean daily temperature of the lake surface and 50 m was greater than 1°C on only 1 out of 40 days between 1st September and 10th October (3%).

The daily moving average (mean) showed a series of cyclical peaks and troughs in lake surface and 1 m temperature data between July and August, with notable peaks occurring on 5th July, 19th July, 26th July, 5th August and 14th August, with a mean inter-peak interval of 11 days (ranging from 8 to 15 days). These features, as well as the intra-seasonal temperature variations described above, are also evident in the shallow observations acquired at ICE-M and ICE-P (Figures 2c–2f).

4.1.2. Longitudinal Variability in Lake Thermal Structure

Shallow observations (lake surface, 1, 5 and 10 m) acquired at all moorings (ICE-D, ICE-M and ICE-P) demonstrate variability in lake temperature with increasing distance from Thulagi Glacier (Figures 3 and 4). We find that mean lake temperatures were consistently warmer closest to the glacier front at ICE-P than furthest from Thulagi Glacier front at ICE-D regardless of depth of the sensor (lake surface, 1 and 10 m) throughout May to October. There is a statistical difference (where Cohen's D is >0.5 , “medium” effect size) between sensors at the lake surface in June (a difference of $0.3 \pm 0.1^\circ\text{C}$), July ($1.0 \pm 0.1^\circ\text{C}$) and October ($0.3 \pm 0.1^\circ\text{C}$), and at 1 m in June ($0.3 \pm 0.1^\circ\text{C}$), July ($0.9 \pm 0.1^\circ\text{C}$), September ($0.2 \pm 0.1^\circ\text{C}$) and October ($0.2 \pm 0.1^\circ\text{C}$) (Table 1). At 10 m depth, there is a statistical difference between temperatures recorded at ICE-P and ICE-D throughout June to October, where Cohen's D increases from 0.69 to 1 in June to 2.29 in October (Table 1). In contrast, there is no statistical difference between lake temperatures observed at ICE-D and ICE-M.

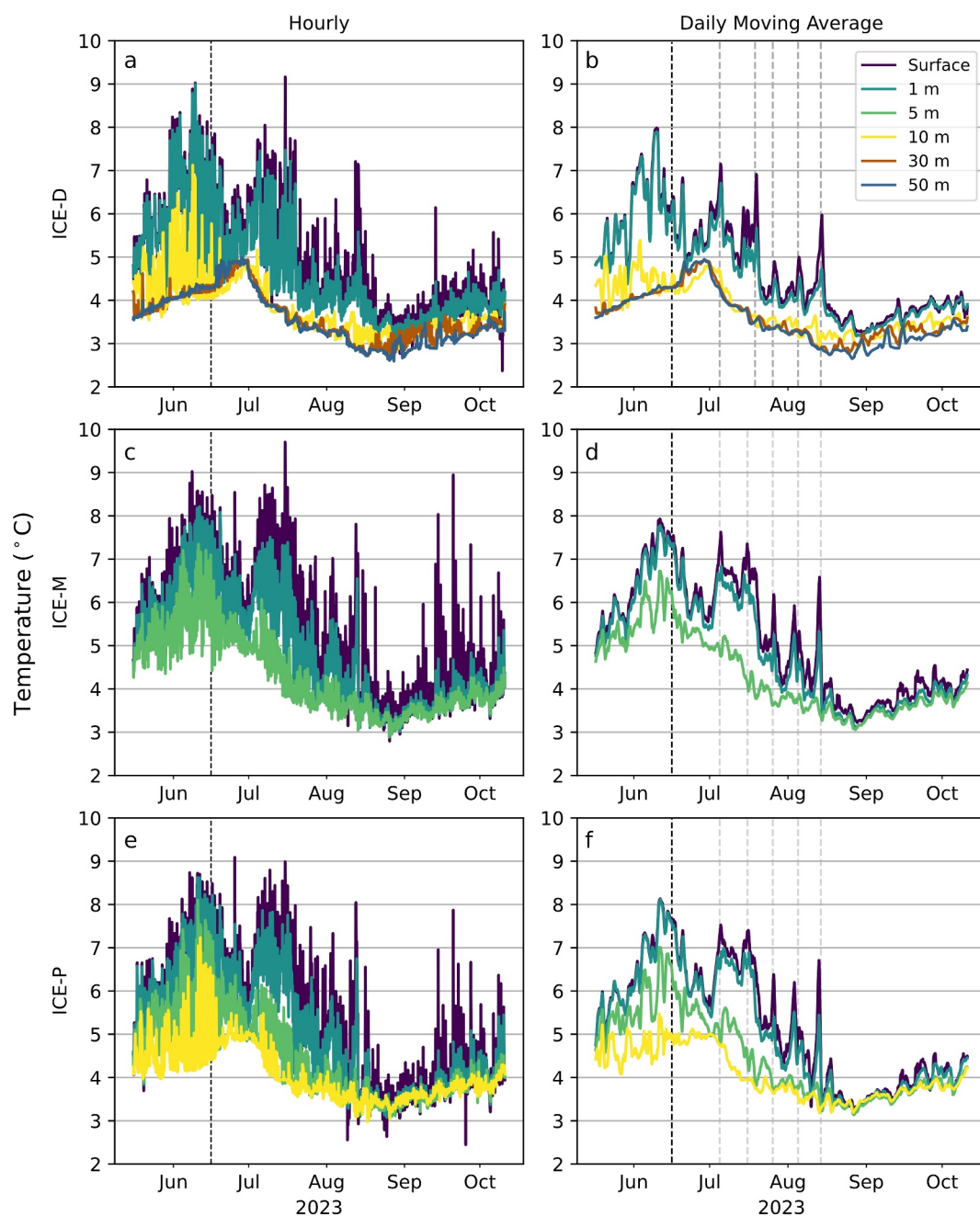


Figure 2. Hourly and daily moving average (mean) lake temperature profiles recorded at ICE-D (a, b), ICE-M (c, d) and ICE-P (e, f) between May and October 2023 at the surface (~10 cm), 1, 10, 30 and 50 m. The black dashed vertical line indicates the onset of the monsoon (14th June 2023). The monsoon withdrew on 14th October 2023, after the end of our observations (DHM, 2024). Dashed vertical lines on (b, d, f) indicate the occurrence of cyclical peaks in lake temperature at all three sensors.

The differences between observations at opposing ends of the lake are most evident when observing the patterns of mean hourly lake temperature (Figure 4). Between May and July, strong diurnal temperature patterns are demonstrated at all three lake locations, although the timing of the diurnal minima and maxima is highly inconsistent between the sites.

During June and July, sensors closest to the glacier front at ICE-P showed opposing temperature patterns at 5 and 10 m to those at the lake surface and 1 m (Figure 4; right panels). For example, in June, mean hourly lake

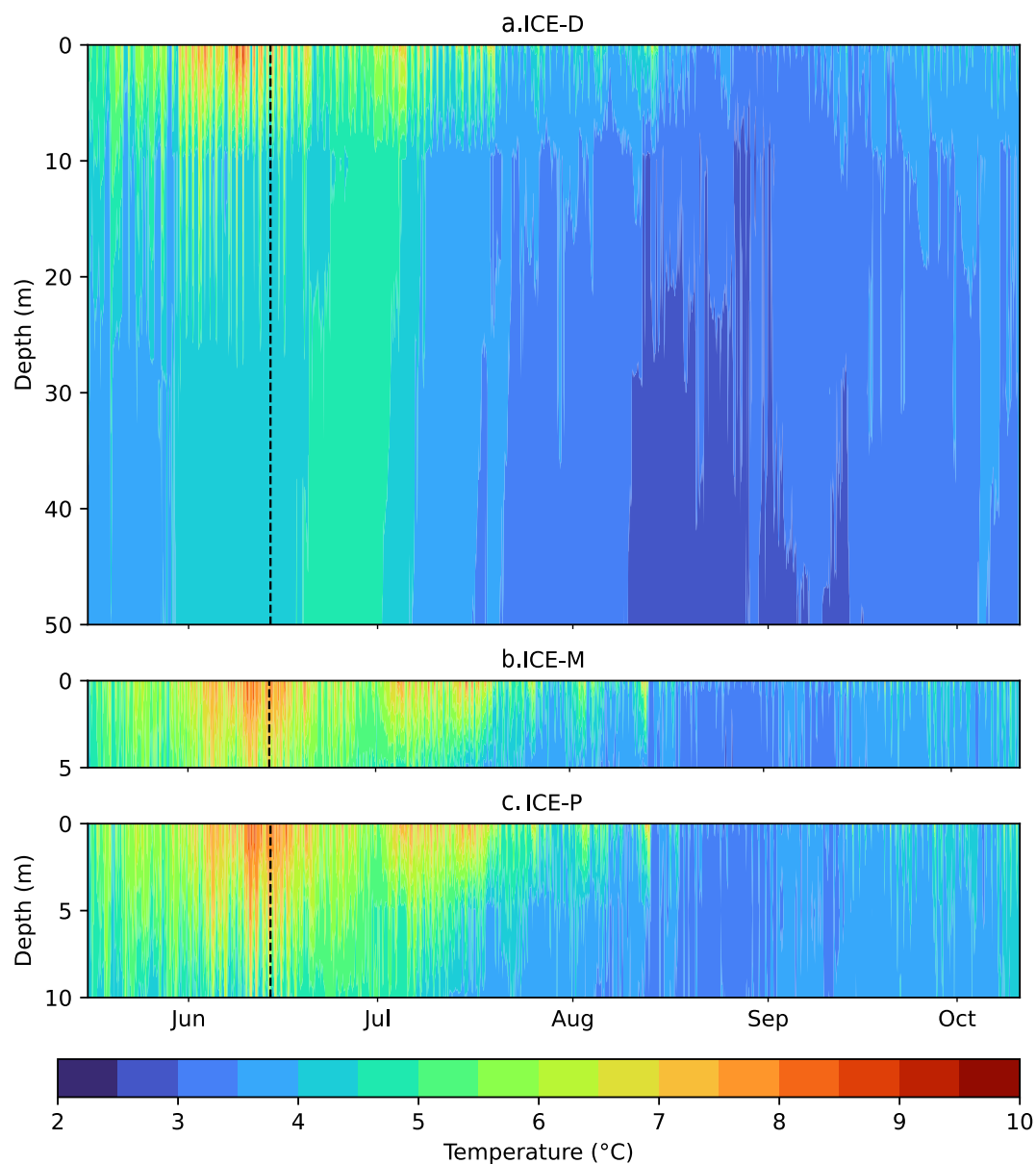


Figure 3. Filled contours of lake temperature profiles recorded at (a) ICE-D (surface to 50 m), (b) ICE-M (surface to 5 m) and (c) ICE-P (surface to 10 m) between May and October 2023. The black dashed vertical line indicates the onset of the monsoon (14th June 2023). The monsoon withdrew on 14th October 2023, after the end of our observations (DHM, 2024).

temperatures at the lake surface and 1 m reached their maxima at 11:00 and 12:00, respectively, coinciding with the timing of minimum mean hourly lake temperatures at 5 and 10 m at 11:00 and 13:00 respectively. At the surface and at 1 m, minimum mean hourly lake temperatures both occurred at 07:00, while at 5 and 10 m, maximum mean hourly lake temperatures occurred at 23:00 and 21:00, respectively. The contrast between sensors at the surface/1 m and at 5 m/10 m is also observed at ICE-M, but negligibly at ICE-D. Here, although the sensors at the surface and at 1 m show similar patterns to those elsewhere, at a depth of 10 m and greater there is negligible evidence of a diurnal temperature pattern throughout the observation period. However, it should be noted that ICE-D was the only mooring where temperature sensors extend beyond depths of 10 m.

From August to October, a weakening of diurnal temperature patterns is evident at ICE-D, ICE-M and ICE-P. Here, peaks in mean hourly lake temperature are evident only at the lake surface and 1 m, with maxima observed around midday, and this pattern is replicated at each site with little variation with distance from the glacier front.

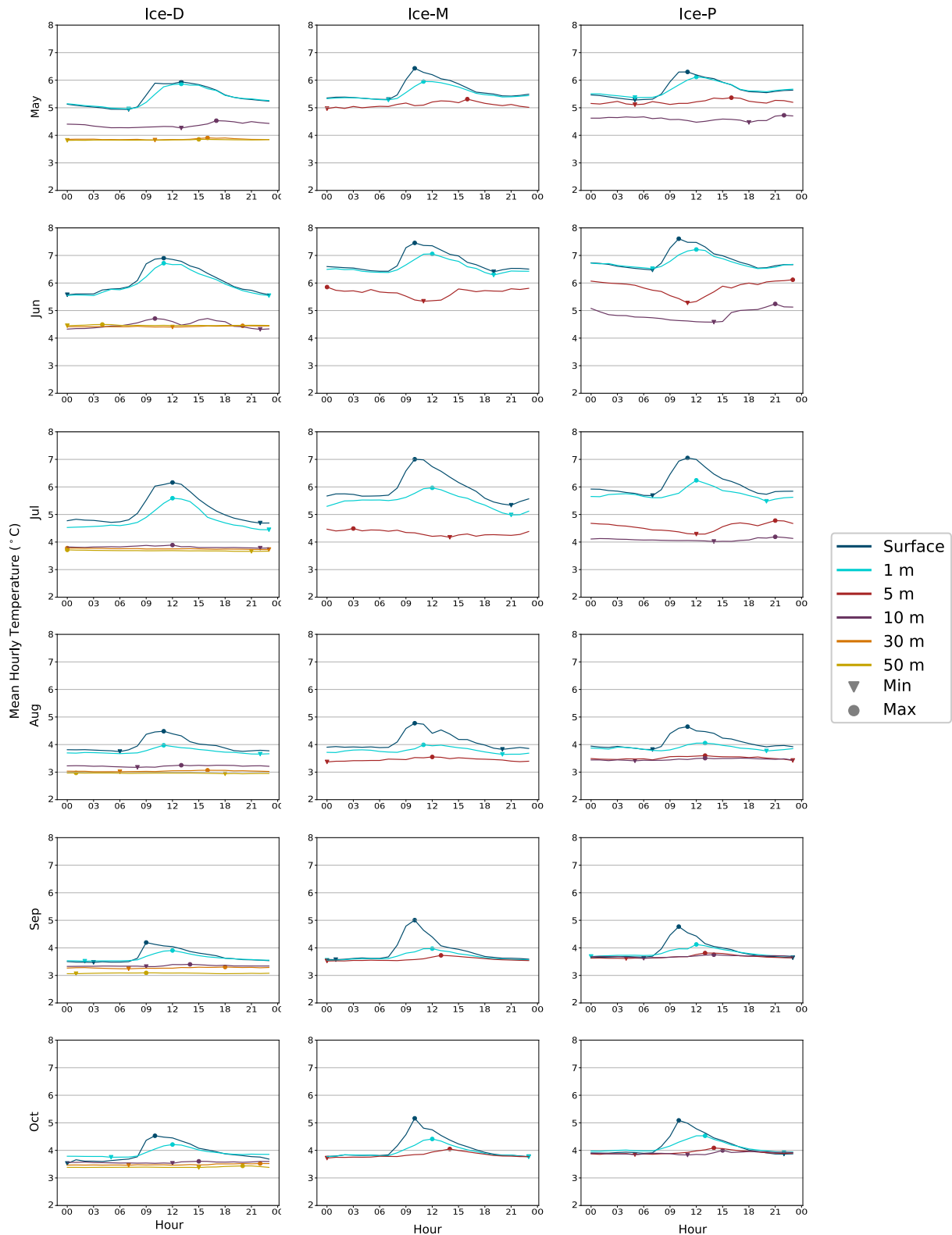


Figure 4. Diurnal plots of mean hourly lake temperature at ICE-D, ICE-M and ICE-P locations (Figure 1) between May and October 2023. Lake temperatures at varying depths are represented by colored lines, and the timing of mean minimum and maximum temperatures are represented by an inverted triangle and circle, respectively.

Table 1
Summary of Differences Between Lake Temperature at ICE-P (Closest to the Glacier Terminus), ICE-M and ICE-D (Furthest From the Glacier Terminus) at Surface, 1, 5 and 10 m Depths by Month

	Surface						1 m			5 m			10 m		
	Mean (°C)	CV (%)	D	Lower (°C)	Upper (°C)	Mean (°C)	CV (%)	D	Lower (°C)	Upper (°C)	Mean (°C)	CV (%)	D	Lower (°C)	Upper (°C)
May ICE-P	5.68	11	–	5.66	5.7	5.66	9	–	5.64	5.68	5.21	8	–	5.19	5.23
ICE-M	5.63	11	0.08	5.61	5.65	5.52	9	0.28	5.5	5.54	5.1	7	0.25	5.08	5.12
ICE-D	5.38	15	0.41	5.35	5.41	5.36	14	0.46	5.33	5.39					
Jun ICE-P	6.84	12	–	6.81	6.87	6.74	12	–	6.72	6.76	5.83	13	–	5.81	5.85
ICE-M	6.74	13	0.11	6.71	6.77	6.57	12	0.21	6.55	6.59	5.65	11	0.26	5.63	5.67
ICE-D	6.09	18	0.75	6.06	6.12	5.98	18	0.8	5.95	6.01					
Jul ICE-P	6.11	18	–	6.08	6.14	5.75	17	–	5.72	5.78	4.55	15	–	4.53	4.57
ICE-M	5.94	20	0.15	5.91	5.97	5.49	18	0.27	5.46	5.52	4.33	13	0.36	4.31	4.35
ICE-D	5.15	22	0.86	5.12	5.18	4.81	19	1	4.78	4.84					
Aug ICE-P	4.09	24	–	4.06	4.12	3.88	18	–	3.86	3.9	3.52	8	–	3.51	3.53
ICE-M	4.1	23	–0.01	4.07	4.13	3.78	17	0.14	3.76	3.8	3.45	8	0.24	3.44	3.46
ICE-D	3.96	18	0.15	3.94	3.98	3.75	12	0.23	3.74	3.76					
Sep ICE-P	3.89	14	–	3.87	3.91	3.82	8	–	3.81	3.83	3.68	6	–	3.67	3.69
ICE-M	3.88	16	0.02	3.86	3.9	3.69	8	0.44	3.68	3.7	3.59	5	0.46	3.58	3.6
ICE-D	3.69	9	0.45	3.68	3.7	3.64	7	0.66	3.63	3.65					
Oct ICE-P	4.17	13	–	4.14	4.2	4.12	8	–	4.1	4.14	3.93	6	–	3.92	3.94
ICE-M	4.1	13	0.12	4.07	4.13	3.96	8	0.5	3.94	3.98	3.83	5	0.45	3.82	3.84
ICE-D	3.92	11	0.51	3.9	3.94	3.9	5	0.78	3.89	3.91	3.57	3	2.29	3.56	3.58

Note. Differences are described through coefficient of variation (CV), effect size (D; Cohen's D), and lower/upper confidence intervals. "D" values in bold indicate where Cohen's D is >0.5 ("medium" effect size) and "D" values underlined and in bold indicate where Cohen's D is >0.8 ("large" effect size). All lake temperature values have an uncertainty of 0.1°C (see Methods).

4.2. Meteorological Conditions

Observations from the AWS show patterns consistent with expected monsoon conditions (Bookhagen et al., 2005; Brunello et al., 2020; Pratap Singh et al., 2020). In May and June, mean daily air temperature increased from a minimum of $2.0 \pm 0.1^\circ\text{C}$ on 20th May to a maximum of $10.4 \pm 0.1^\circ\text{C}$ on 22nd June. Minimum and maximum

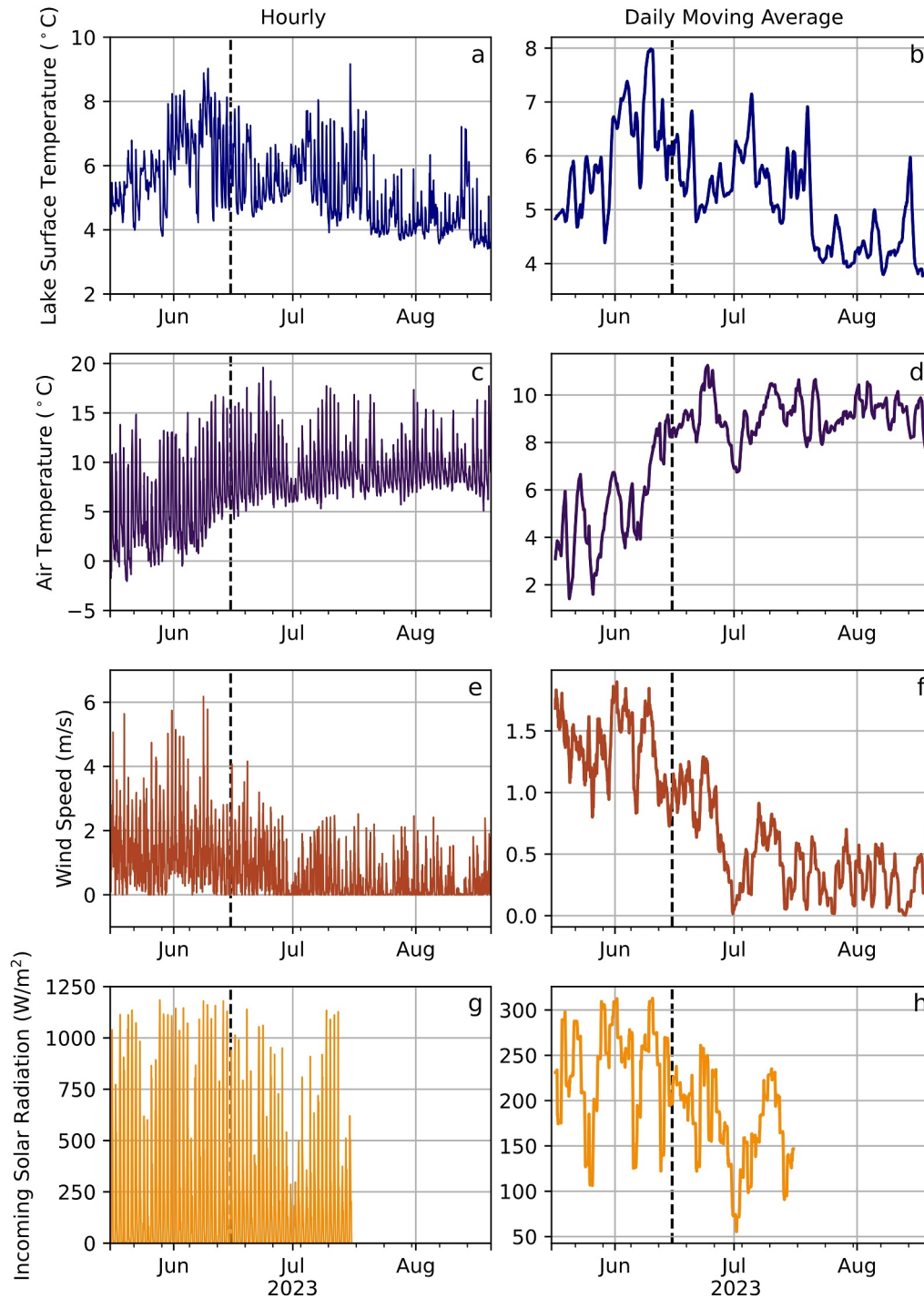


Figure 5. Hourly and daily moving average of lake surface temperature (ICE-D), (a, b) air temperature (c, d), wind speed (e, f) and incoming shortwave radiation (g, h) recorded at an AWS on the true left lateral moraine of Thulagi Lake between 16th May and 19th August 2023. Wind direction, frequency and speeds are located in Figure S6 of Supporting Information S1. The black dashed vertical line indicates the onset of the monsoon (14th June 2023), the monsoon withdrew on 14th October 2023, after the end of our observations (DHM, 2024).

daily air temperatures recorded in May were $-2.5 \pm 0.1^\circ\text{C}$ and $15.1 \pm 0.1^\circ\text{C}$, while in June were $-0.8 \pm 0.1^\circ\text{C}$ and $20.4 \pm 0.1^\circ\text{C}$, with mean diurnal temperatures ranges of 12.4°C and 11.0°C in these months, respectively (Figure 5). Daily mean wind speed demonstrated a contrasting pattern to air temperature during the same period, reducing from 1.7 ± 0.5 m/s on 16th May to 0.04 ± 0.5 m/s on 30th June. Wind speed maxima of 6.47 ± 0.5 m/s and 6.51 ± 0.5 m/s were recorded in May and June, respectively. During the same period, incoming shortwave radiation exhibited mean diurnal ranges of $1,083 \text{ Wm}^{-2}$ in May and 982 Wm^{-2} in June. Maximum and minimum daily mean incoming shortwave radiation in May and June occurred on 20th May and 30th June with readings of $1,236$ and 311 Wm^{-2} , respectively.

In July and August, monthly mean air temperatures were largely consistent at $9.1 \pm 0.1^\circ\text{C}$ and $9.3 \pm 0.1^\circ\text{C}$ respectively. In comparison to May and June, mean diurnal air temperature ranges were lower, at $7.3 \pm 0.1^\circ\text{C}$ and $6.7 \pm 0.1^\circ\text{C}$, and the minimum and maximum air temperatures recorded were $5.2 \pm 0.1^\circ\text{C}$ and $18.3 \pm 0.1^\circ\text{C}$ (July), and $4.9 \pm 0.1^\circ\text{C}$ and $18.9 \pm 0.1^\circ\text{C}$ (August). Wind speeds also plateaued during this period, with daily mean wind speed ranging from 0 to 0.76 ± 0.5 m/s, and maxima of 3.13 ± 0.5 m/s and 2.76 ± 0.5 m/s in July and August, respectively. Incoming shortwave radiation exhibited minimum and maximum mean diurnal ranges of 353 and $1,190 \text{ Wm}^{-2}$ on 1st and 17th July, with a monthly mean diurnal range of 882 Wm^{-2} .

5. Discussion

Observations from Thulagi Lake indicate a complex thermal regime with distinct temporal and spatial variations that deviate from comparable seasonal observations made at non-ice-contact lakes elsewhere in the Himalaya (Sharma et al., 2012) and ice-contact lakes in other glacierised regions of the world (Bird et al., 2022; Sugiyama et al., 2016, 2021). Specifically, we observe a shorter (~ 3 months, with temperatures exceeding 9°C at the lake surface) warm period than in other settings. We suggest that a combination of influx of glacial meltwater and monsoon-specific meteorological conditions drive lake cooling during the glacier melt season.

5.1. Seasonal Evolution of Lake Thermal Structure

From the onset of observations in mid-May to the establishment of the monsoon in mid-June (14th June 2023; DHM, 2024), Thulagi Lake was characterized by strong thermal stratification, where a warmer well-mixed layer of water (epilimnion) formed above a cooler layer (hypolimnion) separated by a thermocline, across which temperature decreases rapidly with depth (Figure 6a; Kirillin & Shatwell, 2016; Wang et al., 2023; Wells & Troy, 2022). Early in the observation period (May), we measured high diurnal temperature ranges in the upper layers ($2.3 \pm 0.1^\circ\text{C}$ at the surface, $1.9 \pm 0.1^\circ\text{C}$ at 1 m and $1.2 \pm 0.1^\circ\text{C}$ at 10 m) compared to low diurnal temperature ranges at depth ($0.2 \pm 0.1^\circ\text{C}$ at 30 m and $0.1 \pm 0.1^\circ\text{C}$ at 50 m). This relative lack of temperature variability at depth suggests that the epilimnion extended to somewhere between 10 and 30 m depth during this time, which is comparable to thermocline depths of 20–25 m reported for Tsho Rolpa in the pre-monsoon period (May to June 1996; Chikita et al., 1999, 2007). The gradual thickening of the epilimnion during this period is most likely related to high wind speeds (~ 6 m/s), inducing vertical mixing of water warmed by high incoming shortwave radiation (Bocaniov et al., 2020; Chikita, 2007; Gorham & Boyce, 1989; Sugiyama et al., 2016; Wang et al., 2023; Wilson et al., 2020).

The establishment of the monsoon in Nepal (mid to late June) coincides with a brief destabilization of the stratified thermal regime. At this time, the epilimnion cools, driven by a reduction in solar radiation, and the hypolimnion warms, driven by heat diffusion across the thermocline (Cowgill, 1967). Water temperatures therefore converge and the lake approaches isothermal conditions (mean temperatures of 5.5°C at the lake surface and 4.7°C at 50 m depth). Although the absolute drivers of the destabilisation are difficult to unravel, it is possible that the persistently high winds (albeit reduced from earlier in the observation period) were sufficient to disrupt the lake structure during this period given the reduction in the thermal density differences between layers.

Between July and August, the thermal regime at Thulagi re-stabilises and remains stratified, but with evident cooling trends of both the epilimnion and hypolimnion. The cooling of the hypolimnion most likely reflects the input of cold, turbid subglacial discharge from Thulagi Glacier, since this is when glacier melt is at its peak, coinciding with rising mean monthly air temperatures. During this period, remotely-sensed surface suspended sediment concentrations (SSCs) (Text S2) increase from an average (mean) of 55.1 mg/L in May and June to 72.4 mg/L in July and August (Table S3 and Figure S4 in Supporting Information S1). This turbid discharge has the additional effect of reducing lake transparency and thus the penetration of solar radiation to greater depths

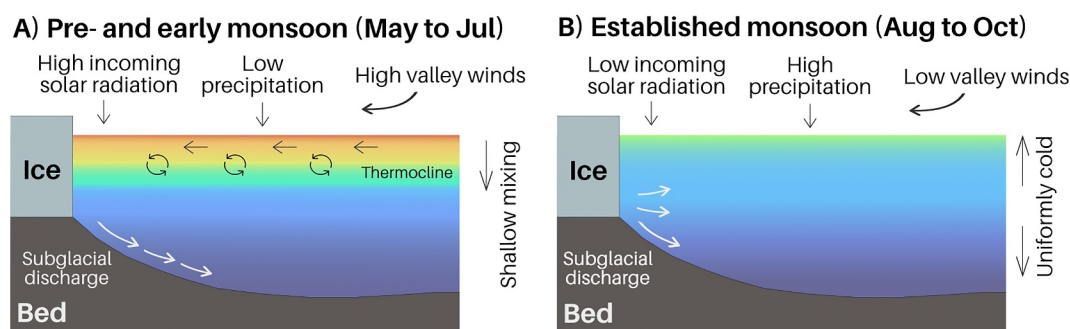


Figure 6. Conceptual figure of thermal conditions at Thulagi Lake, Himalaya during (a) the pre- and early monsoon (May–July) and (b) the established monsoon phase (August–October).

(Kirillin & Shatwell, 2016; Sharma et al., 2012). The reduction in incoming solar radiation, combined with a reduction in mixing potential from declining wind speeds (1.06–0.39 m/s in June and July), most likely led to a more stable, well-stratified structure, as has been observed elsewhere in the region (Chikita et al., 2000; Wang et al., 2023).

While the end of our observations coincided with the withdrawal of the monsoon from Nepal (14th October 2023; DHM, 2024), previous measurements from Thulagi Lake acquired in late October 2017 provide a more complete seasonal picture of the thermal regime. At that time, Watson et al. (2020) observed an inverse thermal structure, where warmest temperatures were observed at the maximum depth (mean temperature of 2.5°C at ~55 m) and coolest temperatures were observed at the surface (mean temperature of 1.8°C), with diurnal mixing events. Inverse thermal regimes are typically associated with winter ice cover, although in this case, it may have reflected a large calving event prior to Watson et al. (2020)'s observations.

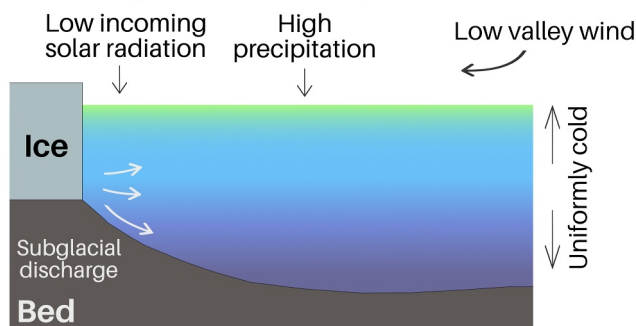
5.2. Drivers of Lake Thermal Regime

The combination of our observations with those of Watson et al. (2020) confirm that Thulagi Lake can be classified as dimictic, with two discrete periods (summer, winter) of stratification (Ficker et al., 2017; Wells & Troy, 2022; Yang et al., 2018). During the pre- and early monsoon phases (May–July), Thulagi's thermal structure and absolute lake temperatures are consistent with historical observations of two other Himalayan ice-contact lakes, Tsho Rolpa and Imja Tsho (Chikita et al., 1999, 2000). Our mean epilimnion temperatures were 5.4–6.1°C at Thulagi (May and June); equivalent temperatures of 5.2°C and 6°C were measured at Tsho Rolpa (late May to early June) and at Imja Tsho (mid-July) respectively. In the pre-monsoon phase, absolute differences of hypolimnion temperatures between Thulagi (4.2°C) and Tsho Rolpa (2.3°C) were small, but still suggest the drivers of thermal structure may differ between sites. In particular, both Tsho Rolpa and Imja Tsho show evidence of sediment-driven thermal structures with temperatures of 2–3°C in the hypolimnion overtopped by 5–6°C in the epilimnion during the pre- and early monsoon phases, but comparable hypolimnion temperatures are not reached at Thulagi until later in the monsoon season (August). This may reflect a difference in the timing and magnitude of sediment-rich meltwater inputs at Thulagi when compared to the other sites. It should also be noted, however, that our deeper temperature sensors were all located at the ice-distal end of the lake, well away from the ice front and the area of maximum sediment influx, which may also partly account for the delayed response.

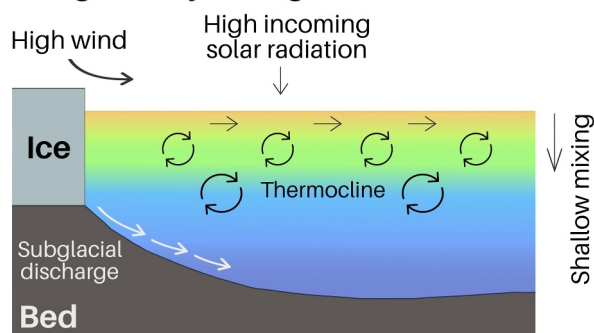
Following this period, the thermal dynamics of Thulagi depart markedly from those that have been described for other dimictic ice-contact lakes around the world (e.g., Lagos Gray, Patagonia; Sugiyama et al., 2021; Figure 7b). In particular, mid-to late-summer periods in dimictic lakes are typically associated with continued surface warming and a gradual deepening of the thermocline until the autumn period (Wang et al., 2023; Wells & Troy, 2022; Yang et al., 2018). In contrast, the latter part of the glacier melt season (August–October) at Thulagi is characterized by cooling in both the epilimnion and hypolimnion, often resulting in isothermal conditions (Figures 6b and 7a). We suggest two key drivers are responsible for this behavior: continued inputs of sediment-rich meltwater, and monsoon-specific meteorological conditions.

Meltwater runoff from Himalayan glaciers peaks during the summer months in response to seasonally warming air temperatures (Zhang et al., 2021, 2024), which coincides with the fastest rates of hypolimnion cooling. The

A) Thulagi Lake, Himalaya (Ice-contact)



B) Lagos Grey, Patagonia (Ice-contact)



C) Idealised (Non-ice-contact)

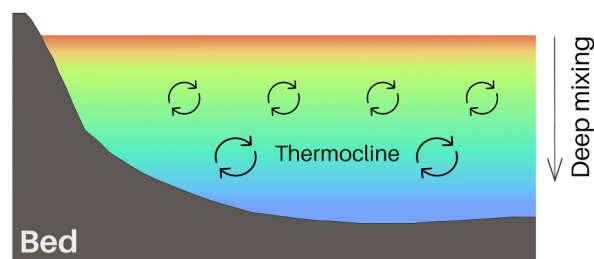


Figure 7. Conceptual figure comparing the thermal conditions of (a) Thulagi Lake, Himalaya during the established monsoon (equivalent to late summer in non-monsoon-influenced regions), with (b) a Patagonian ice-contact lake (Lagos Gray; Sugiyama et al., 2021) and (c) an idealized non-ice-contact lake (adapted from Sharma et al., 2012; Wells & Troy, 2022).

injection of cold and turbid water at depth is highly likely to promote underflows as the subglacial discharge seeks the lowest point in the lake or a location with neutral buoyancy (Carrivick & Tweed, 2013; Dallimore et al., 2003). Thus, these internal currents could additionally contribute to epilimnion cooling through shear and detrainment of the upper and lower stratified layers, as reported elsewhere (Dallimore et al., 2003). It seems unlikely, however, that the input of glacial meltwater is exclusively responsible for cooling at Thulagi, given the severity of epilimnion cooling during this period, and observations from other ice-contact lakes have demonstrated that stratified regimes can persist even through the peak of the glacier melt season (Sugiyama et al., 2016, 2021).

The monsoon is therefore the other possible driver of this late-season behavior. During this period, precipitation is high, solar radiation is low relative to other periods, and wind speed reduces. It is difficult to isolate the effects of these conditions on lake surface energy fluxes but observations from Gokyo Lake, Nepal, which is isolated from any meltwater inputs, provides some useful insights. In contrast to Thulagi, the thermal structure of Gokyo Lake remains stratified throughout the monsoon period, with continued epilimnion warming ($\sim 8^{\circ}\text{C}$ pre-monsoon, $\sim 10^{\circ}\text{C}$ post-monsoon; Sharma et al., 2012; Figure 7c). Although there is some disparity between the respective lake depths that may prevent a direct comparison (Gokyo is 12 m (mean depth) and 16 m (maximum depth) shallower than Thulagi; Sharma et al., 2012), this behavior indicates that while monsoon-specific conditions clearly impact the surface energy balance, they are also probably not the sole driver of ice-contact lake thermal conditions within the region.

From this evidence, we conclude that the influx of glacial meltwater and monsoon-specific meteorological conditions combine to drive the late melt season thermal characteristics of ice-contact lakes like Thulagi. Together, these factors drive lake cooling at depth, and at the surface, such that the stratification period is curtailed compared to elsewhere. The implication is that efforts to incorporate lake effects into numerical models of glacier evolution need to treat those glacier-lake systems located in monsoon regions separately from those elsewhere in the world.

5.3. Short-Term Variations in Thermal Conditions

The series of cyclical peaks and troughs that are evident in the lake surface and 1 m temperature data between July and August coincide with the peak monsoon phase, and particularly strong intraseasonal activity (known as active/break cycles; Annamalai & Slingo, 2001). Active/break cycles result from both westward (10–20 days) and northward (30–60 days) propagating

events and manifest as the spatially and temporally variable distribution of precipitation (Annamalai & Slingo, 2001; Kulkarni et al., 2011). During the active phase of the 10–20 days cycle, which is driven by westward moving convective systems over the Indian Ocean (Kulkarni et al., 2009, 2011), precipitation diminishes over the Nepal Himalaya while intensifying over central India. During the break phase, the pattern is reversed (Karmacharya et al., 2017; Krishnamurthy & Shukla, 2000; Turner & Slingo, 2009).

ERA5 reanalysis data (specifically, total precipitation and incoming solar radiation; Text S3 and Figure S5 in Supporting Information S1), support an interpretation that the peaks and troughs in lake surface temperature observed throughout July and August are driven by these active/break cycles. Following break phases and their associated heavy precipitation events in the region, lake surface temperatures peak (Figure 2, Figure S5 in Supporting Information S1). Owing to the differences in atmospheric and lake temperatures, water vapor condenses at the lake surface, where the resulting latent flux likely serves as an energy source (Miles et al., 2016; Sakai et al., 2000). Furthermore, troughs in lake surface temperature appear to be anti-correlated with peaks in

incoming solar radiation (during active phases, Figure 2, Figure S5 in Supporting Information S1), suggesting that at this time radiation-induced glacier melt is substantial enough to override the typical lake surface warming associated with solar radiation alone.

5.4. Longitudinal Variability in Lake Thermal Conditions

Although partly limited by the absence of temperature measurements at depth at ICE-M and ICE-D, the consistently higher lake temperatures we observe at ICE-P (nearest to the glacier front), than at ICE-D (at the distal end of the lake), are systematic, time-varying, and irrespective of the lake depths observed. This pattern (of warmest water at the ice front) is perhaps counterintuitive and implies a high degree of internal heat convection, during the early part, and up to the peak, of the monsoon. This convection could feasibly be explained by one or more drivers such as wind-driven mixing and/or the presence of underflows.

Longitudinal differences in lake temperature are particularly prominent between May and July in the upper 1 m of the water column (surface and 1 m sensors) (Figures 3 and 4). This coincides with the highest observed wind speeds and solar radiation, both of which are key controls of lake surface warming (Jennings et al., 2012; Wang et al., 2023; Woolway & Simpson, 2017; Wüest et al., 2000). The wind behavior at Thulagi is typical of most glacierised valley environments (Figure S6 in Supporting Information S1), comprising diurnal valley winds which predominantly blow longitudinally along the lake toward the glacier (Chikita, 2007; Jentsch & Weidinger, 2022; Sakai, 2012; Salerno et al., 2023). This scenario serves to promote the advective diffusion of heat toward the glacier terminus (i.e., ICE-P) during the daytime (also observed at Tsho Rolpa; Chikita et al., 1999). Additionally, Thulagi's geometry and surrounding topography also serves to promote greater wind speeds at the ice-proximal end of the lake, enhancing ablation through melt and calving (Sakai & Fujita, 2010), in contrast to the ice-distal end of the lake, where the terminal moraine and dead-ice zone may provide a topographic screening effect, as has been observed at Imja Tsho (Chikita, 2007; Sakai et al., 2009).

This period marks the height of the summer ablation season in the Himalaya (Litt et al., 2019) and so there were meltwater inputs into the lake. Underflows, which arise from the input of cold, turbid subglacial meltwater, will redistribute heat at Thulagi by driving internal circulation currents (Chikita, 1989, 2007; Chikita et al., 1996, 1999). Indeed, Thulagi Lake is characterized by a narrow, longitudinal trough that may promote the generation of underflow currents (Figure S1 in Supporting Information S1; Haritashya et al., 2018), seeking the lowest point in the lake or a location of neutral buoyancy (Carrivick & Tweed, 2013; Dallimore et al., 2003) rather than a large subglacial overdeepening that would inhibit underflow movement (e.g., Sugiyama et al., 2021). Where such underflows exist the epilimnion becomes displaced in the opposite direction, carrying heat in the direction of the ice front. These currents can additionally encourage mixing (and diffusion of heat) through shear and detrainment at the interface of the upper and lower stratified layers (Dallimore et al., 2003).

5.5. Wider Implications of Our Findings

Our results suggest that at Thulagi Lake and other monsoon-influenced ice-contact lakes, the pre- and peak monsoon phases (May–July) are likely the most critical for subaqueous melt-driven frontal ablation at the glacier-lake interface. This short period of combined high lake temperatures (exceeding $9 \pm 0.1^\circ\text{C}$ at the lake surface and a daily mean maximum of $7.98 \pm 0.1^\circ\text{C}$) and stable, stratified lake thermal structure is further intensified by local-scale processes (e.g., underflows, wind-driven mixing) that promote the transport of heat to the glacier front, collectively contributing to ice-melt at the glacier terminus through the positive correlation of subaqueous melt with water temperature (Eijpen et al., 2003; Sakai et al., 2009; Warren & Kirkbride, 2003).

During the pre- and peak monsoon phases, heating that is predominantly within the surface layers also impacts on the rate and style of glacier calving (Carrivick et al., 2020; Mallalieu et al., 2020). Non-uniform melting with depth has been evidenced elsewhere by the protrusion of submerged glacial ice, leading in the longer term to buoyancy-driven subaqueous calving events (Benn & Åström, 2018; Sugiyama et al., 2016). Additionally, the combination of heating at the lake surface and wind-driven wave action promotes the formation of thermo-erosional notches at glacier termini, which leads to overhanging ice and thus subaerial calving (Mallalieu et al., 2020; Röhl, 2006). In non-monsoon-influenced ice-contact lakes, where stratified regimes persist until late summer or autumn (e.g., surface temperatures between 6 and 8°C for Patagonian lakes through austral summer; Sugiyama et al., 2016, 2021), higher rates of subaqueous melt-driven frontal ablation likely persist for the majority of the glacier melt season in line with lake warming (~ 5 months; Sugiyama et al., 2016, 2021).

Contrastingly, we observe that the combination of monsoon conditions and glacier meltwater input ultimately inhibit lake warming (at surface and depth, respectively) over the glacier melt season at Thulagi (~2 months, with reduced mean surface temperatures of ~3.9°C between August and October). Consequently, we infer that sub-aqueous melt-driven frontal ablation processes are likely to be less critical for lake-induced glacier mass loss in monsoon-influenced regions such as the Himalaya, when compared to other glacierised regions globally.

Although studies focusing on the ecosystem services that glacial lakes provide are still relatively few, it is clear that their physical characteristics (i.e., the magnitude and distribution of lake temperatures; the seasonal onset of stratification) exert a strong control on biological and chemical processes, both within the lake itself and downstream (Woolway et al., 2021). For example, thermal stratification influences the transport of oxygen and nutrients between the lake surface and the lake bed and, as such, the vertical distribution and composition of lake biota. These biota play a key role in regulating water quality, and in transferring organic matter through aquatic and terrestrial food webs, moderating nutrient fluxes, and breaking down pollutants (Woolway et al., 2021; Woolway & Merchant, 2019). Moreover, the frequency of overturning, mobilization of lake sediments, and degree of chemical weathering all have important atmospheric ramifications, in particular the extent to which lakes may be sources or sinks of greenhouse gases such as carbon dioxide and methane (Golub et al., 2022; Wang et al., 2023; Woolway et al., 2021; Woolway & Merchant, 2019; Zhu et al., 2024).

Key to advancing this understanding is being able to simulate the future evolution of glacial lakes under different climatic forcings. Although a growing number of observations exist with which to characterize the thermal characteristics of non-glacial lakes (e.g., Tong et al., 2023), there is a comparative dearth of data available within glacierised environments. Current lake evolution models therefore rely on simplified assumptions about lake temperature at depth, the presence or absence of currents, surface meteorological conditions, and lake bed topography, and are largely unable to accommodate the input of cold, sediment-laden water, which as noted at Thulagi likely plays a key role in driving heat circulation especially during the early melt season. Being able to simulate these time-dependent processes would represent an important improvement in both our understanding of physical processes surrounding glacier-lake interaction and our ability to simulate how glaciers respond to proglacial lake development, since they would lead to the calculation of ablation rates through both time and space, and therefore facilitate the inclusion of feedbacks relating to meltwater inputs, lake temperatures, and calving rates, for example. Including these effects in glacier models at a time when glacial lakes are expanding in both number and area (Shugar et al., 2020; Zhang et al., 2024) is highly pertinent.

We recommend that future research focus on obtaining the empirical data necessary to inform such lake evolution models by addressing some of the limitations of this study. In particular, a temporally-complete in situ meteorological data set would enable the use of energy-balance modeling (e.g., Miles et al., 2016) to further assess the climatic drivers of ice-contact lake physical conditions in this region. We also recommend repeating this study design with successful lake temperature observations at increasing lake depths and distances from glacier termini, coupled with time-evolving measurements of turbidity (as a proxy for SSC) and water currents. Ultimately, observations of this nature are necessary at other ice-contact lakes in the monsoon-influenced Himalaya to determine the degree to which findings from Thulagi Lake are generalizable more broadly across the region.

6. Conclusions

We presented the first seasonal measurements of Himalayan ice-contact glacial lake thermal structure at Thulagi Lake, Nepal (4,050 m a.s.l.), acquired over a 5-month period between May and October 2023. Vertical temperature profiles were obtained through the installation of moorings at three locations which encompassed the entire length of the lake. These lake temperature profiles were analyzed for both spatial and temporal patterns, in the context of locally observed meteorological conditions and synoptic climatic phenomena, specifically, the Indian summer monsoon. These data indicate the seasonality of Thulagi Lake throughout the ablation season, when a short, discrete period of relatively high lake temperatures between May and July (maximum temperature of $9.20 \pm 0.1^\circ\text{C}$ and maximum monthly mean of $6.09 \pm 0.1^\circ\text{C}$) was observed. During this period, high diurnal temperature ranges at sensors between the lake surface and 10 m depth suggest higher incoming solar radiation (mean diurnal range of $1,083 \text{ W m}^{-2}$ in May compared to 882 W m^{-2} in July) and higher wind speeds (monthly mean of 1.4 and 1.06 m/s in May and June, respectively) drove convective mixing to between 10 and 30 m depth, leading to stratification for 75% of days observed. Lake temperatures reduced between August and October (maximum temperature of $7.96 \pm 0.1^\circ\text{C}$ and maximum monthly mean of $3.96 \pm 0.1^\circ\text{C}$) coinciding with a

reduction in wind speed (monthly mean of 0.38 and 0.31 m/s in July and August, respectively), leading to stratification in only 3% of days observed.

Our observations highlight the complex seasonal thermal regime of Thulagi Lake driven by both the influx of glacial meltwater and monsoon-specific meteorological conditions (low incoming solar radiation, low wind speeds and high precipitation), resulting in a significant shortening of the summer stratification period (by ~2 months) compared to other glacial and non-glacial dimictic lakes around the world. Despite this important seasonal control, local-scale variations in lake temperature are also evident, likely affected by wind-driven mixing and underflow currents. These factors likely play a role in maintaining consistently higher lake temperatures at sensors nearest to the glacier front compared to at the ice-distal part of the lake (mean differences of 0.3 ± 0.1 to $0.94 \pm 0.1^\circ\text{C}$) and imply a high degree of internal heat convection during the establishing and peak monsoon phases between May and July. We conclude that the establishing and peak monsoon phases are most critical for subaqueous melt-driven frontal ablation processes at Himalayan lake terminating glaciers. During this period, Thulagi glacier was exposed to a short, discrete period of relatively high lake temperatures (maximum temperature of $9.20 \pm 0.1^\circ\text{C}$ and maximum monthly mean of $6.09 \pm 0.1^\circ\text{C}$) intensified by local-scale processes that redistributed heat toward the glacier front, contrasting with similar observations from other glacierised regions. However, our findings also show that monsoon conditions (increased precipitation, reduced incoming solar shortwave radiation and lower wind speed) and the input of glacial meltwater promote lake cooling when observed over the entirety of the glacier melt season, reducing subaqueous melt-driven frontal ablation in high-elevation Himalayan lakes compared to other glacierised regions where stratified regimes persist until late summer or autumn.

Conflict of Interest

The authors declare no conflicts of interest relevant to this study.

Data Availability Statement

The datasets for this study are available online at <https://doi.org/10.5281/zenodo.13913179>. Data on the Indian Summer Monsoon published by Nepal's Department of Hydrology and Meteorology can be obtained its official website (www.dhm.gov.np). ERA5 hourly reanalysis data (including total precipitation and surface solar radiation downwards) are available in Hersbach et al. (2023).

Acknowledgments

ACS is a recipient of a NERC Panorama PhD studentship (NE/S007458/1). DQ acknowledges Rapid Response funding from the University of Leeds. ACS, DQ and NRK were part-funded by the University of Leeds BRAINSTORM ISF project. We thank the Royal Geographical Society (PRA 15.23), Mount Everest Foundation (23-1 ENIGMA), British Society for Geomorphology (BSG-2022-32) and Water@Leeds for their funding support. We thank Nick Pipe from Vortex for supplying the Advanced Elements kayak which facilitated our equipment deployment and collection. Gethin Jones from Sea Kayaking Wales is thanked for his advice and expertise in kayaking training ahead of our expedition. We thank Dan Jantzen, Bob Yoder and Dan Spare for their consultation on Thulagi Lake as a field site. Himalayan Research Expeditions are thanked for facilitating a Nepal Department of National Parks and Wildlife Conservation research permit for fieldwork, in addition to organizing our support team. We thank our expedition guides, Mahesh Magar and Rohan Magar, and our porters who assisted in transporting our equipment to and from the site. We also thank the editor, the associate editor, Prof Chiyan Miao, and two anonymous reviewers for their constructive comments. The authors declare that they have no competing interests.

References

- Annamalai, H., & Slingo, J. M. (2001). Active/break cycles: Diagnosis of the intraseasonal variability of the Asian summer monsoon. *Climate Dynamics*, 18(1–2), 85–102. <https://doi.org/10.1007/s003820100161>
- Benn, D. I., & Åström, J. A. (2018). Calving glaciers and ice shelves. *Advances in Physics X*, 3(1), 1513819. <https://doi.org/10.1080/23746149.2018.1513819>
- Benn, D. I., Warren, C. R., & Mottram, R. H. (2007). Calving processes and the dynamics of calving glaciers. *Earth-Science Reviews*, 82(3–4), 143–179. <https://doi.org/10.1016/j.earscirev.2007.02.002>
- Bird, L. A., Moyer, A. N., Moore, R. D., & Koppe, M. N. (2022). Hydrology and thermal regime of an ice-contact proglacial lake: Implications for stream temperature and lake evaporation. *Hydrological Processes*, 36(4), e14566. <https://doi.org/10.1002/hyp.14566>
- Bocaniov, S. A., Lamb, K. G., Liu, W., Rao, Y. R., & Smith, R. E. H. (2020). High sensitivity of lake hypoxia to air temperatures, winds, and nutrient loading: Insights from a 3-D lake model. *Water Resources Research*, 56(12), e2019WR027040. <https://doi.org/10.1029/2019WR027040>
- Bookhagen, B., Thiede, R. C., & Strecker, M. R. (2005). Abnormal monsoon years and their control on erosion and sediment flux in the high, arid northwest Himalaya. *Earth and Planetary Science Letters*, 231(1), 131–146. <https://doi.org/10.1016/j.epsl.2004.11.014>
- Brun, F., Wagnon, P., Berthier, E., Jomelli, V., Maharjan, S. B., Shrestha, F., & Kraaijenbrink, P. D. A. (2019). Heterogeneous influence of Glacier morphology on the mass balance variability in high Mountain Asia. *Journal of Geophysical Research: Earth Surface*, 124(6), 1331–1345. <https://doi.org/10.1029/2018JF004838>
- Brunello, C. F., Andermann, C., Marc, O., Schneider, K. A., Comiti, F., Achleitner, S., & Hovius, N. (2020). Annually resolved monsoon onset and withdrawal dates across the Himalayas derived from local precipitation statistics. *Geophysical Research Letters*, 47(23), e2020GL088420. <https://doi.org/10.1029/2020GL088420>
- Carrivick, J. L., & Tweed, F. S. (2013). Proglacial lakes: Character, behaviour and geological importance. *Quaternary Science Reviews*, 78, 34–52. <https://doi.org/10.1016/j.quascirev.2013.07.028>
- Carrivick, J. L., Tweed, F. S., Sutherland, J. L., & Mallalieu, J. (2020). Toward numerical modeling of interactions between ice-marginal proglacial Lakes and glaciers. *Frontiers in Earth Science*, 8, 577068. <https://doi.org/10.3389/feart.2020.577068>
- Chikita, K. (1989). A field study on turbidity currents initiated from spring runoffs. *Water Resources Research*, 25(2), 257–271. <https://doi.org/10.1029/WR025i002p00257>
- Chikita, K., Jha, J., & Yamada, T. (1999). Hydrodynamics of a supraglacial Lake and its effect on the Basin expansion: Tsho Rolpa, Rolwaling Valley, Nepal Himalaya. *Arctic Antarctic and Alpine Research*, 31(1), 58–70. <https://doi.org/10.1080/15230430.1999.12003281>

- Chikita, K., Jha, J., & Yamada, T. (2001). Sedimentary effects on the expansion of a Himalayan supraglacial lake. *Global and Planetary Change*, 28(1), 23–34. [https://doi.org/10.1016/S0921-8181\(00\)00062-X](https://doi.org/10.1016/S0921-8181(00)00062-X)
- Chikita, K., Joshi, S. P., Jha, J., & Hasegawa, H. (2000). Hydrological and thermal regimes in a supra-glacial lake: Imja, Khumbu, Nepal Himalaya. *Hydrological Sciences Journal*, 45(4), 507–521. <https://doi.org/10.1080/02626660009492353>
- Chikita, K. A. (2007). Topographic effects on the thermal structure of Himalayan glacial lakes: Observations and numerical simulation of wind. *Journal of Asian Earth Sciences*, 30(2), 344–352. <https://doi.org/10.1016/j.jseas.2006.10.005>
- Chikita, K. A., Smith, N. D., Yonemitsu, N., & Perez-Arllucea, M. (1996). Dynamics of sediment-laden underflows passing over a subaqueous sill: Glacier-fed Peyto Lake, Alberta, Canada. *Sedimentology*, 43(5), 865–875. <https://doi.org/10.1111/j.1365-3091.1996.tb01507.x>
- Cohen, J. (1988). *Statistical power analysis for the behavioral sciences* (2nd ed.). Routledge. <https://doi.org/10.4324/9780203771587>
- Cowgill, U. M. (1967). Heat transfer solely by molecular conduction in the metalimnion. *Proceedings of the national academy of sciences* (Vol. 57(2), pp. 198–200). <https://doi.org/10.1073/pnas.57.2.198>
- Dallimore, C. J., Hodges, B. R., & Imberger, J. (2003). Coupling an underflow model to a three-dimensional hydrodynamic model. *Journal of Hydraulic Engineering*, 129(10), 748–757. [https://doi.org/10.1061/\(ASCE\)0733-9429\(2003\)129:10\(748\)](https://doi.org/10.1061/(ASCE)0733-9429(2003)129:10(748))
- Department of Hydrology and Meteorology, Government of Nepal. (2024). Nepal Climate Summary 2023. Retrieved from https://www.dhm.gov.np/uploads/dhm/climateService/Annual_Summary_20232.pdf
- Eijpen, K., Warren, R. C., & Benn, D. I. (2003). Subaqueous melt rates at calving termini: A laboratory approach. *Annals of Glaciology*, 36, 179–183. <https://doi.org/10.3189/172756403781816158>
- Ficker, H., Luger, M., & Gassner, H. (2017). From dimictic to monomictic: Empirical evidence of thermal regime transitions in three deep alpine lakes in Austria induced by climate change. *Freshwater Biology*, 62(8), 1335–1345. <https://doi.org/10.1111/fwb.12946>
- Furian, W., Loibl, D., & Schneider, C. (2021). Future glacial lakes in high Mountain Asia: An inventory and assessment of hazard potential from surrounding slopes. *Journal of Glaciology*, 67(264), 653–670. <https://doi.org/10.1017/jog.2021.18>
- Golub, M., Thiery, W., Marcé, R., Pierson, D., Vanderkelen, I., Mercado-Bettin, D., et al. (2022). A framework for ensemble modelling of climate change impacts on lakes worldwide: The ISIMIP lake sector. *Geoscientific Model Development*, 15(11), 4597–4623. <https://doi.org/10.5194/gmd-15-4597-2022>
- Gorham, E., & Boyce, F. M. (1989). Influence of lake surface area and depth upon thermal stratification and the depth of the summer thermocline. *Journal of Great Lakes Research*, 15(2), 233–245. [https://doi.org/10.1016/S0380-1330\(89\)71479-9](https://doi.org/10.1016/S0380-1330(89)71479-9)
- Haritashya, U. K., Kargel, J. S., Shugar, D. H., Leonard, G. J., Strattman, K., Watson, C. S., et al. (2018). Evolution and controls of large glacial Lakes in the Nepal Himalaya. *Remote Sensing*, 10(5), 798. <https://doi.org/10.3390/rs10050798>
- Hersbach, H., Bell, B., Berrisford, P., Biavati, G., Horányi, A., Muñoz Sabater, J., et al. (2023). ERA5 hourly data on single levels from 1940 to present. *Copernicus Climate Change Service (C3S) Climate Data Store (CDS)*. <https://doi.org/10.24381/cds.adbb2d47>
- Jennings, E., Jones, S., Arvola, L., Staehr, P. A., Gaiser, E., Jones, I. D., et al. (2012). Effects of weather-related episodic events in lakes: An analysis based on high-frequency data. *Freshwater Biology*, 57(3), 589–601. <https://doi.org/10.1111/j.1365-2427.2011.02729.x>
- Jentsch, H., & Weidinger, J. (2022). Spatio-Temporal analysis of Valley wind systems in the complex Mountain topography of the Rolwaling Himal, Nepal. *Atmosphere*, 13(7), 1138. <https://doi.org/10.3390/atmos13071138>
- Karmacharya, J., New, M., Jones, R., & Levine, R. (2017). Added value of a high-resolution regional climate model in simulation of intraseasonal variability of the South Asian summer monsoon. *International Journal of Climatology*, 37(2), 1100–1116. <https://doi.org/10.1002/joc.4767>
- King, O., Dehecq, A., Quincey, D., & Carrivick, J. (2018). Contrasting geometric and dynamic evolution of lake and land-terminating glaciers in the central Himalaya. *Global and Planetary Change*, 167, 46–60. <https://doi.org/10.1016/j.gloplacha.2018.05.006>
- Kirillin, G., & Shatwell, T. (2016). Generalized scaling of seasonal thermal stratification in lakes. *Earth-Science Reviews*, 161, 179–190. <https://doi.org/10.1016/j.earscirev.2016.08.008>
- Klaar, M. J., Shelley, F. S., Hannah, D. M., & Krause, S. (2020). Instream wood increases riverbed temperature variability in a lowland sandy stream. *River Research and Applications*, 36(8), 1529–1542. <https://doi.org/10.1002/rra.3698>
- Krishnamurthy, V., & Shukla, J. (2000). Intraseasonal and interannual variability of rainfall over India. *Journal of Climate*, 13(24), 4366–4377. [https://doi.org/10.1175/1520-0442\(2000\)013253C0001:IAIVOR253E2.0.CO;2](https://doi.org/10.1175/1520-0442(2000)013253C0001:IAIVOR253E2.0.CO;2)
- Kulkarni, A., Kripalani, R., Sabade, S., & Rajeevan, M. (2011). Role of intra-seasonal oscillations in modulating Indian summer monsoon rainfall. *Climate Dynamics*, 36(5), 1005–1021. <https://doi.org/10.1007/s00382-010-0973-1>
- Kulkarni, A., Sabade, S. S., & Kripalani, R. H. (2009). Spatial variability of intra-seasonal oscillations during extreme Indian monsoons. *International Journal of Climatology*, 29(13), 1945–1955. <https://doi.org/10.1002/joc.1844>
- Lewis Jr, W. M. (1983). A revised classification of Lakes based on mixing. *Canadian Journal of Fisheries and Aquatic Sciences*, 40(10), 1779–1787. <https://doi.org/10.1139/f83-207>
- Litt, M., Shea, J., Wagnon, P., Steiner, J., Koch, I., Stigter, E., & Immerzeel, W. (2019). Glacier ablation and temperature indexed melt models in the Nepalese Himalaya. *Scientific Reports*, 9(1), 5264. <https://doi.org/10.1038/s41598-019-41657-5>
- Mallalieu, J., Carrivick, J. L., Quincey, D. J., & Smith, M. W. (2020). Calving seasonality associated with melt-undercutting and lake ice cover. *Geophysical Research Letters*, 47(8), e2019GL086561. <https://doi.org/10.1029/2019GL086561>
- Miles, E. S., Pellicciotti, F., Willis, I. C., Steiner, J. F., Buri, P., & Arnold, N. S. (2016). Refined energy-balance modelling of a supraglacial pond, Langtang Khola, Nepal. *Annals of Glaciology*, 57(71), 29–40. <https://doi.org/10.3189/2016AoG71A421>
- Mukherjee, S., Joshi, R., Prasad, R. C., Vishvakarma, S. C. R., & Kumar, K. (2015). Summer monsoon rainfall trends in the Indian Himalayan region. *Theoretical and Applied Climatology*, 121(3–4), 789–802. <https://doi.org/10.1007/s00704-014-1273-1>
- Pratap Singh, S., Thadani, R., Gcs, N., Singh, R., & Gumber, S. (2020). The impact of climate change in Hindu Kush Himalayas. *Key Sustainability Issues*, 453–472. https://doi.org/10.1007/978-3-030-29684-1_22
- Read, J. S., Hamilton, D. P., Jones, I. D., Muraoka, K., Winslow, L. A., Kroiss, R., et al. (2011). Derivation of lake mixing and stratification indices from high-resolution lake buoy data. *Environmental Modelling and Software*, 26(11), 1325–1336. <https://doi.org/10.1016/j.envsoft.2011.05.006>
- Röhl, K. (2006). Thermo-erosional notch development at fresh-water-calving Tasman Glacier, New Zealand. *Journal of Glaciology*, 52(177), 203–213. <https://doi.org/10.3189/172756506781828773>
- Saha, P., Mahanta, R., & Goswami, B. N. (2023). Present and future of the South Asian summer monsoon's rainy season over Northeast India. *Npj Climate and Atmospheric Science*, 6(1), 1–11. <https://doi.org/10.1038/s41612-023-00485-1>
- Sakai, A. (2012). Glacial lakes in the Himalayas: A review on formation and expansion processes. *Global Environmental Research*, 16, 23–30.
- Sakai, A., & Fujita, K. (2010). Formation conditions of supraglacial lakes on debris-covered glaciers in the Himalaya. *Journal of Glaciology*, 56(195), 177–181. <https://doi.org/10.3189/002214310791190785>
- Sakai, A., Nishimura, K., Kadota, T., & Takeuchi, N. (2009). Onset of calving at supraglacial lakes on debris-covered glaciers of the Nepal Himalaya. *Journal of Glaciology*, 55(193), 909–917. <https://doi.org/10.3189/002214309790152555>

- Sakai, A., Takeuchi, N., Fujita, K., & Nakawo, M. (2000). *Role of supraglacial ponds in the ablation process of a debris-covered glacier in the Nepal Himalayas* (pp. 119–132). Iahs publication.
- Salerno, F., Guyennon, N., Yang, K., Shaw, T. E., Lin, C., Colombo, N., et al. (2023). Local cooling and drying induced by Himalayan glaciers under global warming. *Nature Geoscience*, 16(12), 1120–1127. <https://doi.org/10.1038/s41561-023-01331-y>
- Sharma, C. M., Sharma, S., Bajracharya, R. M., Gurung, S., Jüttner, I., Kang, S., et al. (2012). First results on bathymetry and limnology of high-altitude lakes in the Gokyo Valley, Sagarmatha (Everest) National Park, Nepal. *Limnology*, 13(1), 181–192. <https://doi.org/10.1007/s10201-011-0366-0>
- Shugar, D. H., Burr, A., Haritashya, U. K., Kargel, J. S., Watson, C. S., Kennedy, M. C., et al. (2020). Rapid worldwide growth of glacial lakes since 1990. *Nature Climate Change*, 10(10), 939–945. <https://doi.org/10.1038/s41558-020-0855-4>
- Sugiyama, S., Minowa, M., Fukamachi, Y., Hata, S., Yamamoto, Y., Sauter, T., et al. (2021). Subglacial discharge controls seasonal variations in the thermal structure of a glacial lake in Patagonia. *Nature Communications*, 12(1), 6301. <https://doi.org/10.1038/s41467-021-26578-0>
- Sugiyama, S., Minowa, M., Sakakibara, D., Skvarca, P., Sawagaki, T., Ohashi, Y., et al. (2016). Thermal structure of proglacial lakes in Patagonia. *Journal of Geophysical Research: Earth Surface*, 121(12), 2270–2286. <https://doi.org/10.1002/2016JF004084>
- Sutherland, J. L., Carrivick, J. L., Gandy, N., Shulmeister, J., Quincey, D. J., & Cornford, S. L. (2020). Proglacial lakes control Glacier geometry and behavior during recession. *Geophysical Research Letters*, 47(19), e2020GL088865. <https://doi.org/10.1029/2020GL088865>
- Tong, Y., Feng, L., Wang, X., Pi, X., Xu, W., & Woolway, R. I. (2023). Global lakes are warming slower than surface air temperature due to accelerated evaporation. *Nature Water*, 1(11), 929–940. <https://doi.org/10.1038/s44221-023-00148-8>
- Turner, A. G., & Slingo, J. M. (2009). Uncertainties in future projections of extreme precipitation in the Indian monsoon region. *Atmospheric Science Letters*, 10(3), 152–158. <https://doi.org/10.1002/asl.223>
- Wang, B., Ma, Y., Wang, Y., Lazhu, Wang, L., Ma, W., & Su, B. (2023). Analysis of lake stratification and mixing and its influencing factors over high elevation large and small lakes on the Tibetan Plateau. *Water*, 15(11), 2094. <https://doi.org/10.3390/w15112094>
- Warren, C. R., & Kirkbride, M. P. (2003). Calving speed and climatic sensitivity of New Zealand lake-calving glaciers. *Annals of Glaciology*, 36, 173–178. <https://doi.org/10.3189/172756403781816446>
- Watson, C. S., Kargel, J. S., Shugar, D. H., Haritashya, U. K., Schiassi, E., & Furfaro, R. (2020). Mass loss from calving in Himalayan proglacial lakes. *Frontiers in Earth Science*, 7, 342. <https://doi.org/10.3389/feart.2019.00342>
- Wells, M. G., & Troy, C. D. (2022). Surface mixed layers in Lakes. In *Encyclopedia of inland waters* (pp. 546–561). Elsevier. <https://doi.org/10.1016/B978-0-12-819166-8.00126-2>
- Wilson, H. L., Ayala, A. I., Jones, I. D., Rolston, A., Pierson, D., de Eyto, E., et al. (2020). Variability in epilimnion depth estimations in lakes. *Hydrology and Earth System Sciences*, 24(11), 5559–5577. <https://doi.org/10.5194/hess-24-5559-2020>
- Woolway, R. I., Maberly, S. C., Jones, I. D., & Feuchtmayr, H. (2014). A novel method for estimating the onset of thermal stratification in lakes from surface water measurements. *Water Resources Research*, 50(6), 5131–5140. <https://doi.org/10.1002/2013WR014975>
- Woolway, R. I., & Merchant, C. J. (2019). Worldwide alteration of lake mixing regimes in response to climate change. *Nature Geoscience*, 12(4), 271–276. <https://doi.org/10.1038/s41561-019-0322-x>
- Woolway, R. I., Sharma, S., Weyhenmeyer, G. A., Debolskiy, A., Golub, M., Mercado-Bettín, D., et al. (2021). Phenological shifts in lake stratification under climate change. *Nature Communications*, 12(1), 2318. <https://doi.org/10.1038/s41467-021-22657-4>
- Woolway, R. I., & Simpson, J. H. (2017). Energy input and dissipation in a temperate lake during the spring transition. *Ocean Dynamics*, 67(8), 959–971. <https://doi.org/10.1007/s10236-017-1072-1>
- Wüest, A., Piepke, G., & Van Senden, D. C. (2000). Turbulent kinetic energy balance as a tool for estimating vertical diffusivity in wind-forced stratified waters. *Limnology & Oceanography*, 45(6), 1388–1400. <https://doi.org/10.4319/lo.2000.45.6.1388>
- Yang, Y., Wang, Y., Zhang, Z., Wang, W., Ren, X., Gao, Y., et al. (2018). Diurnal and seasonal variations of thermal stratification and vertical mixing in a shallow fresh water Lake. *Journal of Meteorological Research*, 32(2), 219–232. <https://doi.org/10.1007/s13351-018-7099-5>
- Zhang, G., Bolch, T., Yao, T., Rounce, D. R., Chen, W., Veh, G., et al. (2023). Underestimated mass loss from lake-terminating glaciers in the greater Himalaya. *Nature Geoscience*, 16(4), 333–338. <https://doi.org/10.1038/s41561-023-01150-1>
- Zhang, G., Carrivick, J. L., Emmer, A., Shugar, D. H., Veh, G., Wang, X., et al. (2024). Characteristics and changes of glacial lakes and outburst floods. *Nature Reviews Earth and Environment*, 5(6), 447–462. <https://doi.org/10.1038/s43017-024-00554-w>
- Zhang, Y., Gao, T., Kang, S., Shanguan, D., & Luo, X. (2021). Albedo reduction as an important driver for glacier melting in Tibetan Plateau and its surrounding areas. *Earth-Science Reviews*, 220, 103735. <https://doi.org/10.1016/j.earscirev.2021.103735>
- Zhu, M., Kuang, X., Song, C., Feng, Y., He, Q., Zou, Y., et al. (2024). Glacier-Fed Lakes are significant sinks of carbon dioxide in the Southeastern Tibetan Plateau. *Journal of Geophysical Research: Biogeosciences*, 129(4), e2023JG007774. <https://doi.org/10.1029/2023JG007774>